

Evolution strategies for parameter optimization in jet flow control

By P. Koumoutsakos, J. Freund¹ AND D. Parekh²

We present results from the application of evolution strategies for parameter optimization in direct numerical simulations and vortex models of controlled jet flows. It is shown that evolution strategies are a portable, highly parallel method that can complement our physical intuition in the parameter optimization of such flows.

1. Introduction

For centuries engineers have taken inspiration from nature in designing efficient aerodynamic configurations. It is no coincidence that the shape of an aircraft's wing resembles a bird's. We wish to approach the problem of flow control, not from the perspective of imitating existing natural forms, but from the perspective of developing efficient control algorithms, by employing techniques inspired by biological processes. These techniques, which we will refer to as "machine learning algorithms", are gaining significance in the areas of modeling and optimization for fluid dynamics problems as a technology that could help reduce cost and time to market of new designs.

1.1 Evolution strategies

Some of the seminal work in this field (Rechenberg 1971, Schwefel 1974, Hoffmeister 1991) actually was aimed at improving aerodynamic shapes. As stated in (Schwefel, 1974):

"In 1963 two students at the Technical University of Berlin met and were soon collaborating on experiments which used the wind tunnel of the Institute of Flow Engineering. During the search for the optimal shape of bodies in a flow, which was then a matter of laborious intuitive experimentation, the idea was conceived of proceeding strategically. However, attempts with the coordinate and simple gradient strategies were unsuccessful. Then one of the students, Ingo Rechenberg, now professor of Bionics and Evolutionary Engineering, hit upon the idea of trying random changes in the parameters defining the shape, following the example of natural mutations. The evolution strategy was born." (The second student was Hans Paul Schwefel).

Since this pioneering work, stochastic optimization techniques have gained recognition and popularity in several fields of engineering, but this has not been the case

¹ University of California, Los Angeles

² Georgia Institute of Technology

in the field of fluid dynamics in the last three decades. Recent work by Rechenberg (1994) focuses on the shape optimization approach with the construction and experimental testing of shapes that have been produced via evolutionary strategies using computer simulations. Evolution strategies have also been implemented in order to optimize the motions of an artificial tuna (M. Triantafyllou, private communication).

Here, we report preliminary results from the application of evolution strategies in the optimization of actuator parameters in active jet flow control and in the optimization of bifurcating and blooming jets.

1.2 Jet flow control

It is desirable in many circumstances to enhance mixing in the exhaust from aircraft engines. Applications include lift enhancement, signature reduction, and temperature reduction on blown flaps. This work focuses on the latter case. The blown flap on a C-17 (Fig. 1) is currently made out of titanium to avoid melting. If mixing can be significantly enhanced so that the plume temperature is reduced, the flap could be constructed from aluminum, a much less heavier and expensive alternative.

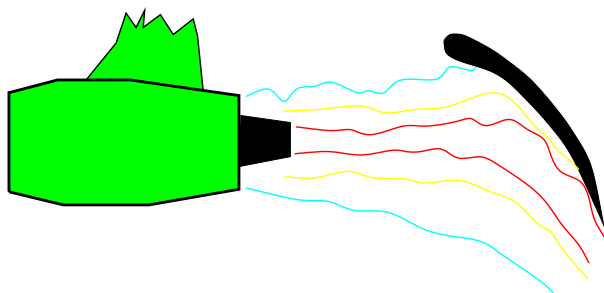


FIGURE 1. Blown flap as on a C-17.

Recently, actuators have been developed and tested on a full-scale engine which have the control authority to accomplish this objective. The goal of this work is to optimize their parameters to maximize their effectiveness. This is being undertaken as a joint experimental, numerical, and control theory effort. The discussion here is limited to the simulations and the application of evolution strategies to the problem.

1.3 Optimization of bifurcating and blooming jets

The proper combination of axial and helical excitation at different frequencies generates the unique class of flows known as bifurcating and blooming jets (Lee and Reynolds 1985, Parekh *et al.* 1987). The axial forcing causes the shear layer to roll up into distinct vortex rings at the forcing frequency. The helical excitation perturbs the rings radially, producing a small eccentricity in the ring alignment. This initial eccentricity is amplified by the mutual ring interactions leading to dramatic changes in jet evolution. When the axial frequency is exactly twice that of the helical excitation, the jet bifurcates into two distinct jets, with successive rings moving alternately on one of two separate trajectories. This Y-shaped jet spreads at angles

over 80 degrees, depending on forcing frequency and amplitude. The relative phase, ϕ , between the axial and helical forcing signals determines the plane in which the jet bifurcates. When the ratio, β , of axial to helical excitation frequency is non-integer, the vortex rings scatter along a conical trajectory. When viewed from downstream, the vortex ring pattern often resembles a bouquet of flowers, hence the name “blooming jet.”

In applying the evolution strategies to this class of flows, we are exploring whether the phenomena discovered experimentally could also be obtained in our simulations via an “evolutionary process” and whether new phenomena could be found. Here a vortex model describes the jet dynamics. The optimization algorithm is tuned to maximize jet spreading by varying the excitation parameters.

2. Evolution strategies for optimization

We discuss first the formulation of evolution strategies for the optimization of N-dimensional functions:

$$F(\mathbf{x}) = F(x_1, x_2, \dots, x_M)$$

We define a vector in the parameter space as an *individual*. The whole discrete parameter space can then be considered as a *population* of individuals. Evolution strategies try to identify the *best* individual from this population based on the *fitness value*, prescribed by the function F . The optimization proceeds by following to a certain extent models of biological evolution.

2.1 Two membered evolution strategies

The simplest (and earliest) form of evolution strategies is based on populations that consist of two competing individuals (“*a two-membered strategy*”). The evolution process consists of the two operations that Darwin (1859) considered as the most important in natural evolution: *mutation* and *selection*. Each individual (i.e. vector in the parameter space) is represented using a pair of floating point valued vectors:

$$\mathbf{u} = \mathbf{u}(\mathbf{x}, \boldsymbol{\sigma})$$

where $\boldsymbol{\sigma}$ is an M-dimensional vector of standard deviations.

Following Rechenberg (1971) and using terminology from biology, the optimization algorithm may be described as follows:

- a - *Initialization*: A parent genotype consisting of M-genes is specified initially (\mathbf{x}^0). At each generation an individual $\mathbf{u}_p^n = (\mathbf{x}_p^n, \boldsymbol{\sigma}_p^n)$ is identified.
- b - *Mutation*: The parent of generation-n produces a descendant, whose genotype differs slightly from that of the parent. The operation of mutation is then realized by modifying \mathbf{x} according to:

$$\mathbf{x}_c^n = \mathbf{x}_p^n + \mathcal{N}(0, \boldsymbol{\sigma}_p^n) \tag{2.1}$$

where $\mathcal{N}(0, \boldsymbol{\sigma})$ denotes an M-dimensional vector of random Gaussian numbers with zero mean and standard deviations $\boldsymbol{\sigma}$.

c - *Selection*: Due to their different genotypes the two individuals of the population can have a different fitness for survival. This fitness is evaluated by the function f . Only the fittest of the two individuals is allowed to produce descendants at the following generation. Hence to *minimize* F we write:

$$\mathbf{x}_p^{n+1} = \begin{cases} \mathbf{x}_p^n, & \text{if } F(\mathbf{x}_p^n) \leq F(\mathbf{x}_c^n); \\ \mathbf{x}_c^n, & \text{otherwise.} \end{cases} \quad 2.2$$

Note that in this two-membered algorithm the vector σ of standard deviations remains unchanged throughout the evolutionary process.

For *regular optimization problems* (see Michalewicz, 1996 for a definition) it is possible to prove the convergence of the method to a global minimum. However, this theorem does not provide a convergence rate of the method.

In this work we have implemented the *1/5 success rule* proposed by Rechenberg (1971). According to this rule: *During the optimum search the frequency of successful mutations is checked periodically by counting the ratio of the number of successes to the total number of trials. The variance is increased if this ratio is greater than 1/5 and it is decreased if it is less than 1/5.* The period over which this performance is being checked depends on the number of parameters that are being optimized. We refer to Schwefel (1995) for further details on the implementation of the two-membered evolution strategies.

2.2 Multi-membered evolution strategies

One of the drawbacks of the 1/5 rule for the two-membered strategy is that it may lead to premature convergence, as the step lengths can be reduced to zero, thus not improving the progress towards a global optimum. There are several possible remedies to this drawback. Of particular interest are those that can be constructed by further developing the model of evolution to resemble natural processes. In that context, a higher level of imitation of an evolutionary process can be achieved by increasing the number of members in a population. Such multi-membered strategies are usually formulated in terms of μ -parents and λ -descendants. The most common strategies are then described as (μ, λ) and $(\mu + \lambda)$. In the (μ, λ) case at each generation the μ -fittest individuals are selected only among the λ children of the generation, whereas in the $(\mu + \lambda)$ case the parents are also included in the evaluation process. Schwefel (1995) presents an extensive comparison of multi-membered and two-membered evolution strategies for a series of optimization problems.

2.3 Handling of constraints

One of the advantages of evolution strategies is the ease and simplicity by which they can handle problem constraints. Such constraints are usually formulated as inequalities. For example in the case of q constraints of the parameters \mathbf{x} we require that:

$$C_j(\mathbf{x}) \geq 0 \quad \text{for all } j = 1, \dots, q$$

Descendants of a certain parent that do not satisfy the constraints are accounted as results of unsuccessful mutations. Occasionally the boundaries of the constrained

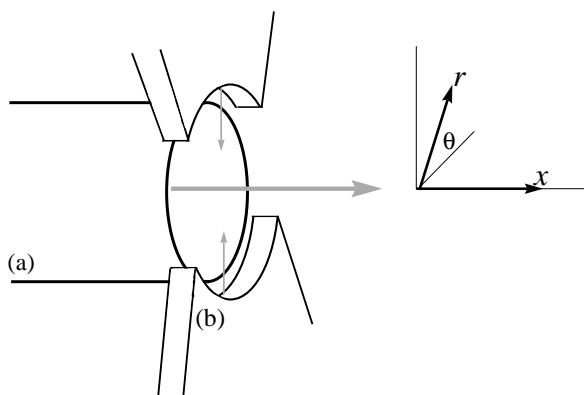


FIGURE 2. Schematic shows the nozzle (a) and actuators (b).

regions are smoothed out in order to facilitate the convergence of the method in highly constrained problems.

3. Jet flow control

The compressible flow equations were solved with direct numerical simulation using a combination of sixth order compact finite differences, spectral methods, and fourth order Runge Kutta time advancement. Further details of the numerical algorithm and techniques for including actuators into the calculations were recently reported by Freund & Moin (1998). Naturally, in a direct numerical simulation we are restricted to highly simplified geometries (Fig. 2); nevertheless, the actuators were able to reproduce the effects observed in experiments by Parekh *et al.* (1996). Figure 3 shows a visualization of a jet forced into a flapping mode and an unforced jet. Clearly, the mixing is enhanced downstream.

For this preliminary study, only three types actuation parameters were varied: the amplitude, frequency, and phase. The actuation was a simple waveform sum of harmonic waveforms:

$$v_r = \sum_{i=1}^N A_i \left(1 + \sin \left(\frac{U St_i}{D} t + \phi_i \right) \text{sgn}(\cos(\theta)) \right), \quad 3.1$$

where v_r is the radial velocity at the actuator exit and A_i are the amplitudes, St_i are the Strouhal numbers, and ϕ_i are the phases of the different modes. The $\text{sgn}(\cos(\theta))$ causes each waveform to excite a flapping mode in the jet. Note that the phases, ϕ_i , are the relative phases of the different modes setting the two actuators always at 180° out of phase. The flow rate out of either actuator was constrained to be less than $U/2$ where U is the jet velocity. This was accomplished by simply “clipping” the velocities to be below this level.

The only constraint on A_i was that they be non-negative. Strouhal numbers were restricted to be $0 \leq St \leq 0.8$ and the phases were constrained to be $\phi_i \in [0, 2\pi]$.

A very low Reynolds number ($Re = 500$) jet at Mach 0.9 was simulated in this preliminary effort to minimize the computational expense. The computational mesh

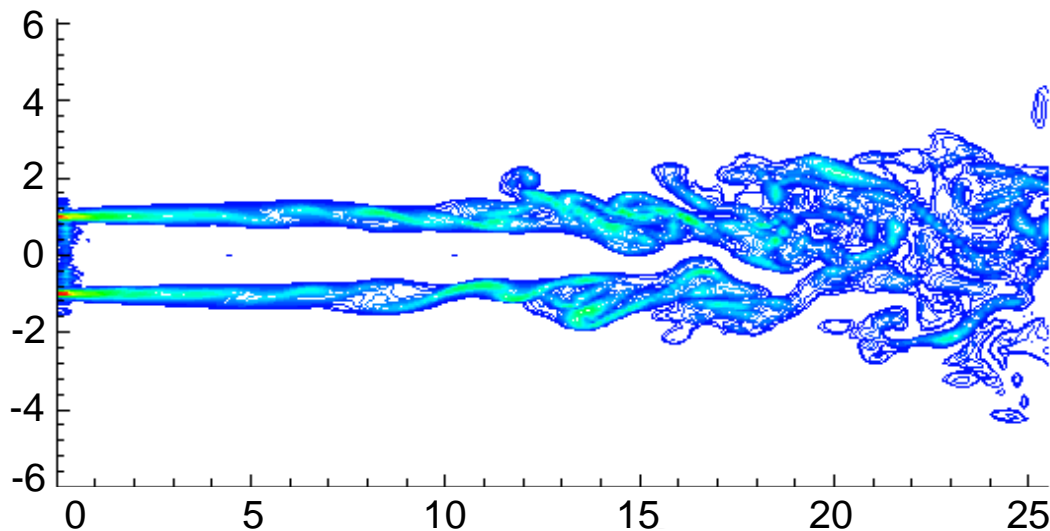


FIGURE 3A. Unforced turbulent jet. Visualization of vorticity magnitude.

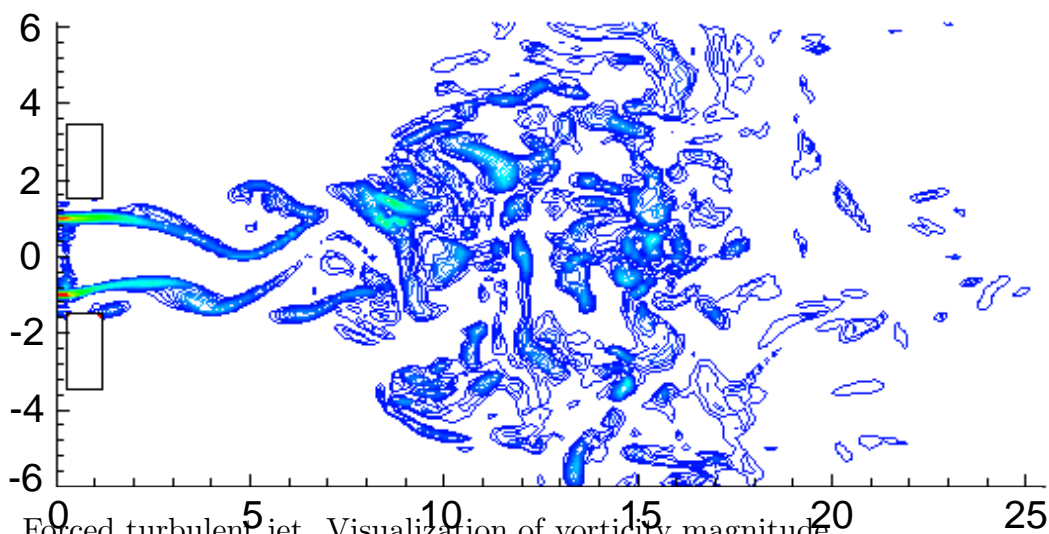


FIGURE 3B. Forced turbulent jet. Visualization of vorticity magnitude.

was $112 \times 42 \times 16$ in the streamwise, radial, and axial direction respectively and the computational domain extended to 16 radii downstream and 5 radii in the radial direction. A stretched-mesh boundary zone was positioned outside of the region to cleanly absorb fluctuations convecting out of the domain. In each iteration of the evolution strategy, the jet was simulated starting from an unforced case for several periods of forcing after the passing of initial transients. Because the flow becomes quasi-periodic, this was sufficient to provide a measure of the long-time actuator effectiveness. Each iteration required approximately 10 minutes and in total 200 iterations were made (the best case was found after approximately 150 iterations).

Three wave forms ($N = 3$) were used and the initial control parameters were

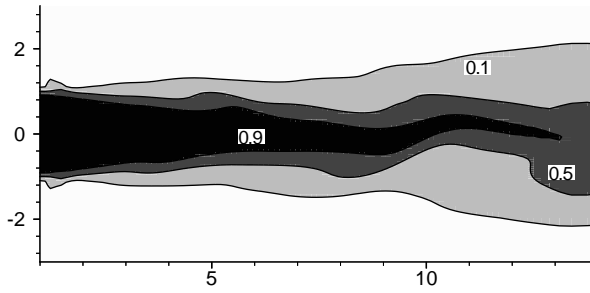


FIGURE 4A. Jet mixture fraction for the first guess parameters.

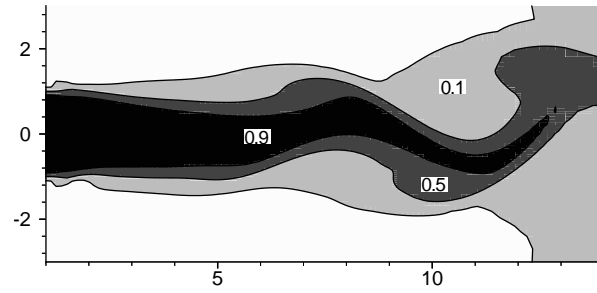


FIGURE 4B. Jet mixture fraction with the best case parameters after 200 iterations.

A_i/U	St_i	ϕ_i
0.45	0.5	0.0
0.40	0.2	0.7
0.35	0.5	1.0

The goal set for the evolution strategy was to maximize

$$Q = \int_0^\infty \int_0^{2\pi} \int_{4r_o}^{8r_o} v_r^2 r dr d\theta dx.$$

This metric Q , was increased by over a factor of 10 from the initial case by the best case parameters:

A_i/U	St_i	ϕ_i
0.04	0.33	0.54
0.42	0.17	0.31
0.07	0.45	1.57

It is interesting to note that the evolution strategy “chose” to reduce the amplitude of two of the wave modes to a very low level. Effectively, it found the same *ad hoc* scheme that was shown to be successful by Parekh *et al.* (1996) and Freund & Moin (1998). A forced and unforced case are visualized in Fig. 4. The best case clearly shows a high amplitude flapping mode which would greatly enhance mixing downstream.

4. Vortex model of bifurcating and blooming jets

In this work we model a circular jet by the combination of discrete vortex filaments and a semi-infinite cylindrical sheet of vorticity. The cylindrical sheet models the nozzle source flow whereas the ring filaments model the vortex rings generated by the axial excitation of the shear layer.

The semi-infinite sheet of vorticity extends from $-\infty$ to the origin. Its axis defines the jet centerline, and the end of the sheet is identified with the jet exit. The helical excitation used in the experiments of Lee and Reynolds (1985) is modeled

by rotating the axis of the vortex cylinder about the nominal jet centerline. The displacement, A_h , of the jet centerline from the nominal centerline corresponds to the amplitude of excitation, and $\bar{A}_h \equiv A_h/R$. The rotation frequency is given by:

$$f_h = \frac{f_a}{\mathcal{R}_f}, \quad 4.1$$

where the orbital frequency is defined as:

$$f_a = St_a \frac{\gamma}{D}, \quad 4.2$$

The frequency f_a is the rate at which filaments are generated at the origin.

The interaction of the vortex sheet with the filaments is assumed to be such that the sheet influences the motion of the filaments but the filaments do not influence the sheet. The velocities induced by each filament and by the jet function are superimposed to determine the trajectory of each filament. The Strouhal number sets the time between creation of new ring filaments at the origin.

The circulation of each filament is identical and is determined from circulation conservation constraints. Assuming the thickness of the cylindrical sheet to be much smaller than its radius, the vorticity flux (per unit of circumference) within the sheet through any plane perpendicular to the jet's axis is given by $U^2/2$. By the assumption of a perfect fluid, the vorticity convected from the cylindrical sheet must equal the vorticity convected by the discrete filaments. This conservation relation can be expressed in terms of Γ and γ as

$$\frac{\Gamma}{\Delta t} = \frac{\gamma^2}{2}, \quad 4.3$$

where Γ is the circulation of each ring filament, γ is the circulation per unit length of the cylindrical vortex sheet, and Δt is the time between generation of ring filaments. By Eqs. 4.8 and 4.9, one obtains

$$\gamma = St_a \frac{\Gamma}{R}. \quad 4.4$$

Further details concerning the applicability of this model and its numerical implementation are reported in Parekh *et al.* (1988).

4.1 Parameter optimization using evolution strategies

The primary parameters that govern the jet evolution St_a , β (frequency ratio of axial and orbital excitation), A_a , A_h , and ϕ . The effect of the axial excitation, A_a , is approximated by generating distinct vortex rings at the axial forcing frequency. The sensitivity to axial forcing amplitude is not modeled. In these simulations the other four parameters are allowed to vary over the following ranges: $0 \leq A_a \leq 1$, $0.1 \leq St_a \leq 1$, $0.2 \leq \beta \leq 5$, $0 \leq \phi \leq 2\pi$. Different flow patterns can be observed with variations in β for fixed values of the other parameters. The simulation is able

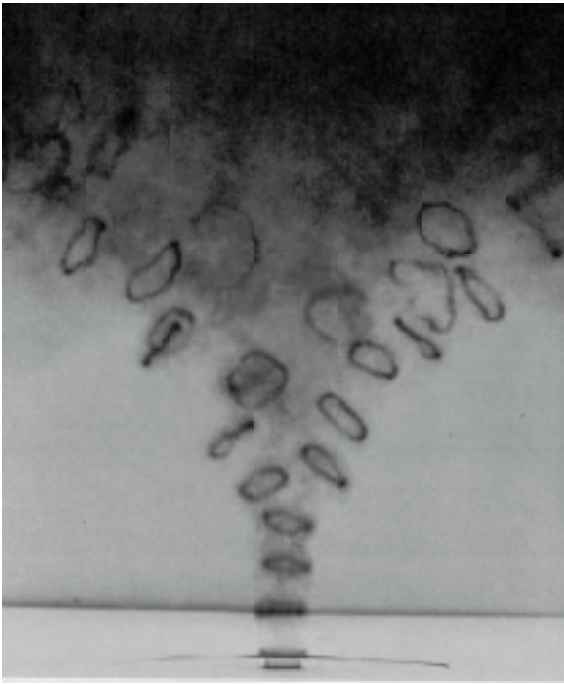


FIGURE 4.1A. Blooming jets: Experimental Results of Lee and Reynolds (1985): $\beta = 1.7$, $A_h = 0.04$, $St_a = 0.46$, $Re = 4300$.

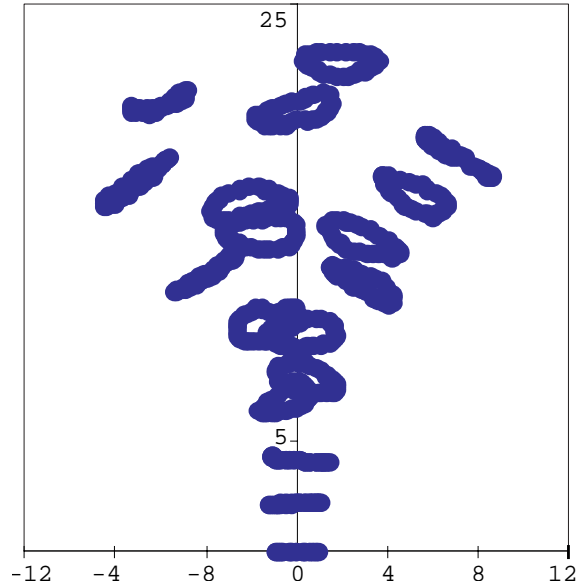


FIGURE 4.1B. Blooming Jets: Simulations $\beta = 1.7$, $A_h = 0.05$, $St_a = 0.55$.

to represent qualitatively the full range of jet phenomena observed in experiments, including bifurcating and blooming jets (Fig. 4.1).

For the optimization, several metrics for jet spreading angle were considered, including the average radial displacement of the vortex elements, jet spreading angle, and ring trajectory angles. We also considered amplitude normalized formulations of these metrics to account for the cost of excitation. The metrics were evaluated over a broad range of test cases to check if they would be robust enough to provide the proper relative rating over the parameter space considered. Some metrics are artificially biased by the initial displacement of the rings or by normalization with very small excitation amplitudes. One metric that is both simple and effective for this simulation is the average angle of the nominal ring trajectories. For each case, this metric is evaluated after the same number of periods (typically, eleven) of axial excitation. The nominal ring trajectory angle, θ , is defined as the angle between the jet centerline and the line that connects the center of the jet exit to the centroid of the vortex ring nodes.

Starting with an initial guess for each of these parameters and constraints on the range of values allowable for each parameter, the genetic algorithm searches to optimize jet spreading. The scope of this work did not allow for an exhaustive investigation of the parameter space and convergence characteristics, but even these preliminary simulations yielded promising results. With all four parameters varied simultaneously, the genetic algorithm selects a blooming jet similar to what has

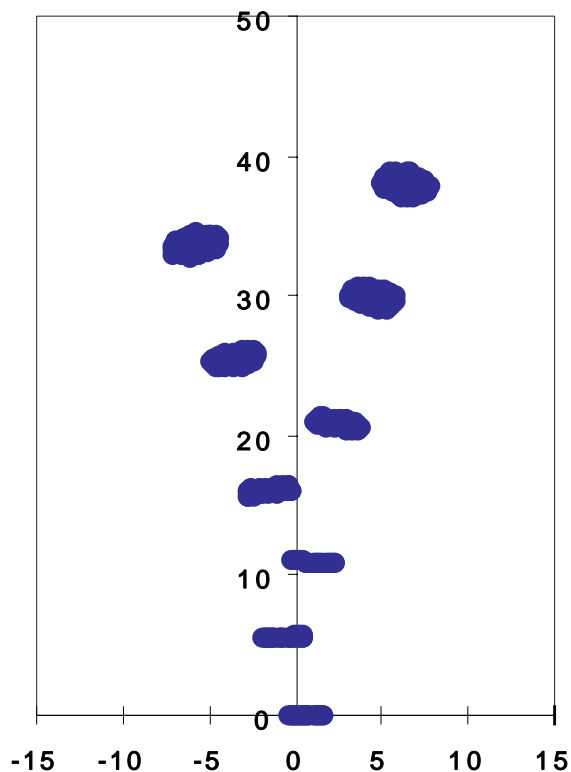


FIGURE 4.2A. Hybrid bifurcating jet with $St_a = 0.28$, $A_h = 0.63$, $\beta = 2$, and $\phi = 0$ (side view).

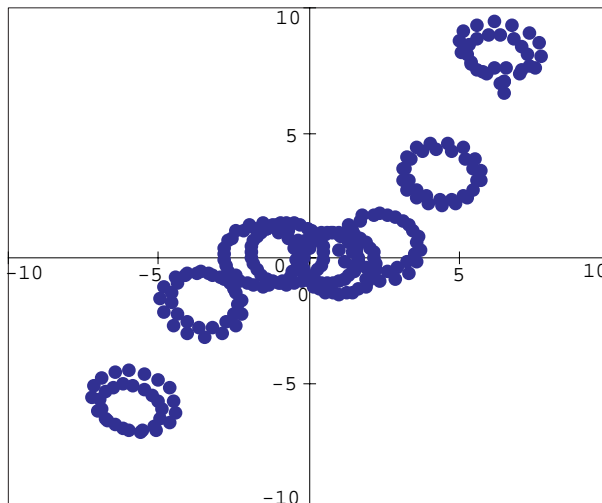


FIGURE 4.2B. End view. Each ring's 32 nodes are plotted as solid circle.

been observed in experiments.

The most striking result was found when we constrained $\beta = 2$ and kept ϕ fixed. Initially we expected the algorithm to select a bifurcating jet similar to Fig. 4.1A with values of St_a and A_h that maximize the spreading angle. Instead, a unique jet flow (Fig. 4.2) was found that had never been observed in previous experiments or calculations. This jet flow initially resembles a bifurcating jet. Several diameters downstream, however, the two branches of the jet exhibit a secondary bifurcation in which the rings change direction along a path with an azimuthal angle about $\pi/4$ different from their original trajectory. This results in a wide spreading angle as seen in Fig. 4.2B.

The simulation often has difficulty providing valid solutions for $St_a > 0.4$ since the initial ring filaments get tangled together and quickly degrade to an unrealistic state. This constraints were implemented in the evolution strategy by simply considering these cases as unsuccessful tries for the optimization algorithm.

5. Summary and conclusions

These preliminary results from the application of evolution strategies to the problem of flow control suggest that stochastic optimization can be a valuable tool that can complement physical understanding and deterministic optimization techniques.

As a closing remark, we quote from Schwefel:

Since according to the “No-Free-Lunch” (NFL) theorem (Wolpert and Macready, 1996) there cannot exist any algorithm for solving all optimization problems that is on average superior to any competitor, the question of whether evolutionary algorithms are inferior/superior to any alternative approach is senseless. The NFL theorem can be corroborated in the case of EA versus many classical optimization methods insofar as the latter are more efficient in solving linear, quadratic, strongly convex, unimodal, separable, and many other problems. On the other hand, EA’s do not give up so early when discontinuous, nondifferentiable, multimodal, noisy, and otherwise unconventional response surfaces are involved. Their robustness thus extends to a broader field of applications, of course with a corresponding loss of efficiency when applied to the classes of simple problems classical procedures have been specifically devised for.”

Hence, in the realm of flow control, the key issue is the identification of a suitable optimization method for the specific problem in hand. The portability, ease of parallelization, and the results reported herein and in (Müller et al. 1999), suggest that EA’s present a powerful technique for parameter optimization in problems of flow control.

REFERENCES

- DARWIN, C. 1859 *The origin of species by means of natural selection*.
- FREUND, J. B. & MOIN, P. 1998 *Mixing enhancement in jet exhaust using fluidic actuators: direct numerical simulations*, ASME FEDSM98-5235.
- HOFFMEISTER F. & BÄCK T. 1991 Genetic algorithms and evolution strategies: Similarities and differences. Proc. of 1st International Conference on Parallel Problem Solving from Nature, Berlin. *Springer*.
- LEE, M. & REYNOLDS, W. C. 1985 Bifurcating and blooming jets. *Fifth Symp. on Turbulent Shear Flows*, Ithaca, New York. 1.7–1.12.
- MICHALEWICZ, Z. 1996 *Genetic Algorithms + Data Structures = Evolution Programs*. Springer-Verlag Berlin.
- MÜLLER, S. MILANO, M. & KOUMOUTSAKOS, P. 1999 Evolution strategies for turbulent channel flow control using rotors. (in preparation).
- PAREKH, D. E., REYNOLDS, W. C. & MUNGAL, M. G. 1987 Bifurcation of round air jets by dual-mode acoustic excitation. *AIAA 87-0164*.
- PAREKH, D. E. 1988 Bifurcating jets at high Reynolds numbers. *PhD thesis*. Department of Mechanical Engineering, Stanford University.
- PAREKH, D. E., KIBENS, V., GLEZER, A., WILTSE, J. M. & SMITH, D. M. 1996 Innovative jet flow control: mixing enhancement experiments. *AIAA Paper 96-0308*. 34th Aerospace Sciences Meeting and Exhibit
- RECHENBERG, I. 1971 *Evolutionstrategie - Optimierung technischer Systeme nach Prinzipien der biologischen Evolution*. Fromman-Holzboog.

- RECHENBERG, I. 1994 *Evolution Strategy '94*, Frommann-Holzboog, Stuttgart.
- SCHWEFEL, H. P. 1974 *Numerische Optimierung von Computer-Modellen*. Birkhäuser, Basel.
- SCHWEFEL, H. P. P. E. 1995 *Evolution and Optimum Seeking*. Wiley Interscience.
- WOLPERT, D. H. & MACREADY, W. G. 1996 No Free Lunch Theorem for Search. *Technical Report SFI-TR-95-02-010*, Santa Fe Institute.